

DRAG COEFFICIENT OF SINGLE SPHERICAL PARTICLE

IN DRAG REDUCING POLYMER FLUIDS,
معامل المقاومة الجزيئات كروية في مخلول بوليمر
مخفض للاحتكاك

L. H. Rabie, and M. M. Kamel²

Mechanical Engineering Dept., Faculty of Engineering,
Mansoura University, Mansoura, 35516, EGYPT.

² Mechanical Engineering Dept., Faculty of Engineering,
Cairo University, Cairo, EGYPT.

ملخص البحث.

البحث يقدم دراسة معمليه لمقاومة اجسام كروية صلبه للحراره في مائع مخفض الجرا الاحتكاكي من محاليل بولي-اكريلاميد ذات تركيزات مختلفه. تم قياس معامل المقاومة بقياس السرعه النهايه لسقوط تلك الاجسام في المائع بواسطه جهاز مزود بهاميرا للتصوير السريع عند سرعه 1000 لقطه في الثانيه. توضح النتائج ان معامل مقاومه الاجسام الكروية الصلبه في محاليل البولي-اكريلاميد اقل بصفة عامه منها في الموائع النيوتونيه ولكن عند القيم الصغيره لرقم رينولدز فان معامل المقاومة يكون اكبر لمحاليل البولي-اكريلاميد. وقد امكن استنتاج علاقته تربط بين التغير في معامل مقاومه الاجسام الصلبه في محاليل البولي-اكريلاميد مخفضه الجرا الاحتكاكي مقارنه بالموائع النيوتونيه مع رقم رينولدز Reynolds ورقم ويسنبرج Weissenberg او معامل Polymer-particle parameter.

ABSTRACT.

An experimental study for the drag of solid spheres in drag reducing fluids is presented. Polyacrylamide solutions of different concentrations are considered. The drag coefficient is measured by the terminal velocity of the spherical particle falling in stagnant fluid using high speed camera. Compared to Newtonian fluid results, the drag of solid particle in polymer solutions exhibit reduced values. However, a drag increase is exhibited at low Reynolds number. Analysis of the data show the presence of a critical Reynolds number that distinguish between the drag increase and drag reduction regions. It has been postulated that the measured drag is a result of two opposing effects of polymer additives. One is flow resistance increase due to increased extensional viscosity. The other, is the reduction in the form drag due to the influence of these additives on vortex shedding and boundary layer separation. It has been found that the experimental data of drag coefficient is best correlated with the polymer-particle parameter ϕ or Weissenberg number W_s as well as Reynolds number.

1. INTRODUCTION.

The flow of non-Newtonian, viscoelastic drag reducing fluids, have received wide attention from fluid mechanics scientists for two reasons. First, is due to recent development in industrial technology which brought such fluids into practical use. Second, is that the presence of few parts per million of high molecular weight polymers or flexible fibres in the turbulent flow reduce the frictional drag drastically. Therefore, numerous investigations have been published [1-2]. Most of them are directed to understand the phenomena, while others into direct practical applications. Two-phase flow of bubbles, droplets and particles in turbulent flow are encountered in many of these applications. They may include drilling of tunnels or boreholes, hydraulic transportation, floatation, fluidization, dust and drop precipitation, sedimentation, particle separation and many other industrial processes. Erosion is a problem that associates the two-phase flow of particles, and strongly related to particle dynamics in the flow. The drag between phases plays an important role in particle dynamics of such fluid flows.

Very little work have been directed to the two-phase flow of drag reducing fluids. The addition of drag reducing additives to turbulent suspension flows has been investigated by Poreh et al [3], Ghassemzadeh et al [4], Pollert [5] and Golda [6]. The experimental results show that, the addition of polymers to liquid-solid suspensions turbulent flow reduce the friction drag similar to single phase flow. They exhibit high sensitivity to mechanical degradation. Similar work was carried by Matthys et al [7] for friction and heat transfer in clay suspension flow with 20 wppm polymer additives. Their results exhibited characteristics typical of the viscoelastic solutions. However, the influence of polymer additives on particle-turbulence interaction has not yet been known.

Many theoretical and experimental studies are carried out on particle dynamics in Newtonian fluids. Clift et al [8] present comprehensive review for the dynamic behavior of bubbles, drops, and particles in different flow fields. The experimental data of the drag of spherical particle in steady Newtonian fluid flow are correlated to Reynolds number and presented in the standard drag curve shown in figure (1) [9]. Lee [10] studied the drag coefficient of spherical particles in turbulent two-phase suspension flow. It is established that the particle drag can be described by the simple Stokes law, based on an apparent turbulent viscosity of the fluid for the particles in the suspension flow. However Gore et al [11] stated that the drag coefficient is best represented by the standard drag curve. Liu et al [12] investigated the drag coefficient of single droplets moving in infinite droplet chain on the axis of a tube. Drag coefficient was measured via the measurements of the terminal velocity using LDA [12]. Their results show that the drag coefficient of droplets is one order of magnitude less than that of single droplet. Hetsroni [13] investigated the interaction between solid particle and the turbulence of the carrier fluid. Review of available experimental data suggested that particles with low Reynolds number cause suppression of the turbulence, while particles with higher Reynolds number cause enhancement due to wake shedding. Huang et al [14] show that, drag coefficient of moving drop experiencing condensation is the resultant of friction, pressure and condensation drag.

Ni et al [15] studied the turbulent diffusivity of small particles in pipe flow of dilute air-solid suspensions. They show that turbulent diffusion is governed by the fluid-particle interaction. It was found that the product of particle diffusivity and inverse relaxation time, which is function of particle drag, is almost constant. Berlemont et al [16] used a Lagrangian approach to describe particle dispersion in turbulent flows. It shows that particle trajectories are affected by drag coefficient. Govan [17] shows that turbulent diffusion coefficient of large particles reduces to very simple form which is function of drag coefficient. Ruck et al [18] studied particle dispersion in a single-sided backward facing step flow using LDA. The results show that particle diffusion differs from the eddy diffusion even in the range of micron-sized particles.

Previous discussion show that, particle dynamics has been extensively studied in Newtonian fluids. Very little data are available for particle dynamics in non-Newtonian fluids. Most of them were carried out in clay or kaolin-water suspensions. Such type of structurally viscous fluid is Rheologically considered a Bingham fluid. Valentik et al [19] measured the settling velocity of spheres in kaolin suspensions. Du Plessis et al [20] measured the settling velocity of glass spheres and sand particles in clay-water suspensions. Pazwash et al [21] measured the drag coefficient of spheres and different shaped bodies in clay-water suspensions. Dedegil [22] analyzed available experimental data of drag coefficient and settling velocity of particles in non-Newtonian suspensions. Slattery and Bird [23] determined the drag coefficient of spheres in CMC polymer solutions by measuring the settling velocity. This work is the only available in drag reducing viscoelastic fluids. Others were carried out on flow around cylinder [24-27]. Kit et al [24], James et al [25], Fruman et al [26], and Kato et al [27] investigated the drag and the pressure distribution on circular cylinders in polymer solutions. Their data covers a wide range of Reynolds number. This work presents an experimental study for the drag and settling velocity of spherical particles in drag reducing Polyacrylamide solutions.

2. EXPERIMENTAL TECHNIQUES.

The object of this work is to study the influence of drag reducing additives upon the drag of spherical particle. The experimental technique considered in this work to measure the drag on solid particle is a direct one. The drag coefficient is measured by the terminal velocity of the falling particle in a stagnant fluid. The terminal velocity is measured using a high speed camera.

The experiments are carried out by dropping spherical stainless steel particle into stagnant fluid in a glass tank of 20x40 cm² base and 60 cm height. Test solution level is kept at 50 cm from the tank base. The high speed camera is focused on a view of 6 cm height. The view was 52 cm down the test solution level in the tank. This ensures constant velocity of the falling particles. This was examined by measuring the fall velocity at different distances from the liquid level in the tank. Figure (2) shows that constant fall velocity is achieved at 25 - 35 cm from the level of test solution. The tank dimensions are large enough to ensure that the distance between the falling particle and the wall is sufficient so that the wall has no effect on the settling motion. The motion of the falling

particles is recorded in tapes using the data acquisition system of the high speed camera. Recorded data are played back to study the particle motion and to measure the fall time of the particle using the digital timer of the data acquisition system. The fall velocity is measured by the time taken by the particle to fall 6.0 cm. The speed of the camera was fixed at 1000 fps (frames per second). This allows the timer of the data acquisition system to have a resolution of 0.0001 sec. Spherical particles of 13 different sizes with diameter range of 3.2 mm to 25.4 mm are used throughout this work. Test solutions considered are 10, 25, 50, 100, 140, 500 and 1000 wppm Polyacrylamide solutions as well as water. The viscosity of Polyacrylamide solutions is measured and presented in figure (3). It shows that the viscosity ratio of polymer solutions to that of the solvent " μ/μ_s " is almost linear with polymer concentration "C" in wppm. The best fit of our data is given by

$$\mu / \mu_s = 1.0 + 0.0021 C$$

For a particle falling in viscous fluid, it reaches its steady state movement after a certain time (distance). The steady state condition is to be attained when the gravity force W, buoyancy force A, and drag force D are in equilibrium, and the particle has a constant fall velocity U. Hence, the drag force is given by

$$D = W - A \quad (1)$$

where,

$$W = g \cdot \rho_p \cdot (D_p)^3 \cdot \pi / 6$$

$$A = g \cdot \rho_f \cdot (D_p)^3 \cdot \pi / 6$$

and,

$$D = C_D \cdot \rho_f \cdot U^2 \cdot (D_p)^2 \cdot \pi / 4$$

Arrangement of equation (1) gives the drag coefficient C_D as function of the fall velocity U as,

$$C_D = (4/3) \cdot (\rho_p / \rho_f - 1) \cdot g \cdot D_p / U^2 \quad (2)$$

Equation (2) can be rewritten as

$$C_D = (4/3) \cdot (Re)^2 / Ar$$

where,

$$Re = \text{Reynolds number} = U \cdot D_p \cdot \rho_f / \mu, \text{ and}$$

$$Ar = \text{Archimedes number} = (D_p)^3 \cdot g \cdot (\rho_p / \mu)^2 / (\rho_p / \rho_f - 1)$$

4. RESULTS.

The results of the fall velocity measurements using high speed camera adjusted at 1000 fps are presented as function of the particle diameter in figure (4). It shows that the data are best fitted by logarithmic curve. For drag reducing fluids, experimental data show that spherical particles has higher fall velocities compared to Newtonian ones. The fall velocity of drag reducing fluids increases with polymer concentration to reach its maximum value at 50 wppm, then, it decreases with concentration. A value

of more than 45% increase in fall velocity is found to associate 50 wppm Polyacrylamide solution. However, results of 1000 wppm solution exhibit lower fall velocity values compared to water for small particle sizes, and higher values for large particle sizes. It worthy to mention that in this work each data point is the result of an average of 5 experimental values.

The experimental results of drag coefficient C_D of spherical particle in Newtonian (water) and drag reducing additive fluids are presented in figure (5). The results of the drag coefficient are compared with the well known standard curve for Newtonian fluids and presented in figure (5-a). The results of drag coefficient using the high speed camera are slightly lower than the standard curve. However, the agreement is generally well. In fact, our experimental data covers Reynolds number range of 4×10^2 - 4×10^4 . That range is characterized by unsteady vortex formation behind the sphere and constant angle of flow separation. Hence, a constant value of drag coefficient is found.

The experimental data of drag coefficient of spherical particles in drag reducing polymer solutions are shown in figures (5-b), (5-c), and (5-d) as function of Reynolds number. Seven Polyacrylamide solutions, 10, 25, 50, 100, 140, 500, and 1000 wppm are considered. In general, drag reducing fluids data exhibit lower drag coefficient compared to water results. For the range of Reynolds number "Re" considered, the 50 wppm Polyacrylamide solution has the minimum drag coefficient of about 50% less than water. For each polymer concentration, the drag coefficient decreases with Reynolds number to a minimum value and then increases with further increase in Reynolds number. For concentrated polymer solutions, 1000 wppm a remarkable drag increase in drag coefficient at low Reynolds number is found. The drag coefficient data are plotted as function of Polyacrylamide concentration for particle diameters 3.2, 4, 5.6, 6.4, 8.4, 10.3, 12.7, 14.3, 15.9, and 25.4 mm respectively in figure (6). These data show that the drag coefficient of dilute solutions is, generally, lower than that of concentrated solutions for all particle sizes.

5. DISCUSSION.

In the experimental data presented in this work, the influence of drag reducing additives upon the drag of spherical particles is shown. Remarkable reduction of the particle drag in polymer solutions compared to Newtonian fluid is exhibited at high Reynolds number and dilute polymer solutions. However, an increase in drag is found at low Reynolds number of the spherical particles, and concentrated solutions. Noticeable scatter in the experimental data is also found.

It has been experimentally verified by many investigators (28) that drag reducing additives in small concentrations can cause serious effects in flows which are essentially non-turbulent and steady. Such effects have been observed in flow patterns with high strain rate regions, as the flow near the stagnation point of blunt bodies, pitot tube nose, small orifice and small cylinders. Pitot tube measurements in polymer solutions exhibit anomalous impact pressure results even in dilute solutions. Both drag and pressure distribution measurements of viscoelastic fluid flow on circular cylinders are presented in (24-27). Compared to Newtonian fluids, results exhibit drag increase at low Reynolds number and drag reduction at high

Re. This is in agreement with our results of spherical particles. Pressure distribution measurements show lower pressure values in the neighborhood of the stagnation point and a downstream shift of the separation point. The measured pressure in the intermediate and separation zones are very close to those of Newtonian fluid with delayed separation [26-27].

The drag of spherical particle in Newtonian fluid is a function of particle's Reynolds number. However, for drag reducing viscoelastic fluids at least one additional parameter must be introduced to account for the non-Newtonian characteristics of such fluid. It is well known that polymer solutions, is characterized by relaxation time θ which is independent of concentration and is given by [29];

$$\theta = 50 \mu_s \cdot [\mu] \cdot M / (RT) \quad (3)$$

and

$$[\mu] = 1.25 \times 10^{-2} \cdot (M)^{0.78} \quad (4)$$

where, μ_s is the solvent viscosity, $[\mu]$ is the intrinsic viscosity, M is the molecular weight of polymer molecules, R is the universal gas constant and T is the solution temperature.

The additional parameter may be suggested as a polymer-particle one, that correlates the characteristics of polymer solution and particles. It may be determined by the dimensionless parameter ϕ defined as.

$$\phi = \theta \cdot \dot{\gamma} / (D_p)^2 \quad (5)$$

It relates the shear viscosity and relaxation time θ of polymer solution to the particle diameter. Such parameter was considered by Klt et al [24], and James et al [25] to analyze their experimental data of circular cylinders. Introducing this parameter in our analysis, many trials have been made to correlate ϕ with our experimental results. The best of these trials which has minimum scatter is to plot the change in drag coefficient δC_D ($\delta C_D = 1 - C_D/C_{D\omega}$) divided by ϕ as function of particle's Reynolds number. Figure (7) presents such correlation. For the range of Reynolds number and particle size considered in this work, the best fit of such data representation is given by the linear relation;

$$\delta C_D / \phi = 0.64682 Re - 2.1893 \times 10^3 \quad (6)$$

Another dimensionless parameter that may be considered to correlate the strain rate of the flow on the sphere with polymer solution parameter. It is known as Weissenberg number "Ws" which is defined as;

$$Ws = \theta \cdot U / D_p \quad (7)$$

It has been found that the experimental data is best represented by plotting the change in drag coefficient of the spherical particles due to polymer additives δC_D divided by Weissenberg number "Ws" as function of particle's Reynolds number Re. As shown in figure (8), the best fit of the experimental data is given by the logarithmic relation,

$$\delta C_D / Ws = 0.224 \ln(Re) - 1.711 \quad (8)$$

Both correlations given by (7) and (8) show that for drag reducing fluids, there is a critical value for particle's Reynolds number Re^* . For particles with Reynolds number lower than that value, an increase in drag coefficient is exhibited, while a reduction in particle's drag occurs at higher Reynolds number. It looks very similar to drag reduction onset criteria of turbulent pipe flow of drag reducing additive fluids.

In order to interpret the reported experimental results, it is very useful to understand the behavior of polymer molecules in the flow. It is well known that the molecules of flexible, long chain, and high molecular weight polymers, are present in a random coiled state in the solution. As these molecules are subjected to a straining motion, of a certain minimum value, they elongate increasing the flow resistance. Such increase in flow resistance is represented by the increase in extensional viscosity of the solution. The critical strain rate, at which polymer molecules elongate, depends on polymer type. As the strain rate increases with the increase in Reynolds number, polymer molecules stretch more and more such that they reach their maximum value when all polymer molecules are fully extended. Hence, the extensional viscosity increases very rapidly with strain rate to a maximum value of several orders of magnitude higher than Newtonian fluid value. Accordingly, the flow around the sphere suffers from increase in flow drag due to increased extensional viscosity of polymer solution.

On the other hand, as shown in pressure distribution measurements on the surface of circular cylinders [26-27], drag reducing polymer additives affect boundary layer development and delay its separation and so reduce the form drag. Increasing Reynolds number, further delay in boundary layer separation occurs and further reduction in form drag is achieved. The flow around the sphere is almost similar to that around the cylinder. Hence, the influence of drag reducing additives on the form drag of spherical particles is similar to that of circular cylinders.

It has been experimentally verified that the vortex structure in the wake of solid sphere is distinguished into three regions [9]. Stationary ring-vortex for $20 < Re < 130$, where a vortex ring that has a stable position on the back of the sphere and a stable boundary with the surrounding fluid. Unsteady ring vortex for $130 < Re < 450$, where, the vortex ring suffers a periodic fluctuating motion around the stagnation point on the back of the sphere. For $Re > 450$, the unsteady vortex ring breaks down and unsteady single vortex appears, where, a periodic formation and detachment of the vortices occurs. The presence of polymer molecules in the flow inhibit the shedding of the unsteady vortices into the wake. Frequency reduction of such vortices implies a reduction of the form drag of the sphere. Polymer molecules influence vortex shedding when the time scale of such unsteady vortex structure is comparable to the time scale of polymer additives.

The above discussion shows that drag reducing polymer additives have two opposite effects on the flow around solid sphere. One is the increase in flow resistance on the sphere due to increased extensional viscosity of such fluid flows. This effect dominates low Reynolds number range. Second is the reduction of the form drag due to the influence of additives upon vortex shedding and delay of boundary layer separation. This effect is much pronounced at high Reynolds number. Hence, at any value of Reynolds number, the value of drag on a solid particle in drag reducing polymer solution depends on the contribution of the two opposite effects to drag.

6. CONCLUSIONS.

An experimental study for the drag of solid spheres in drag reducing polymer solutions is presented. Dilute and concentrated Polyacrylamide solutions with concentration ranges from 1 to 1000 wppm are considered in this work. The drag coefficient is experimentally measured by the terminal velocity of a falling particle using high speed camera. Particle's drag in polymer solutions exhibit lower values compared to those of Newtonian fluid. While, the results show higher values at low Reynolds number and concentrated polymer solutions. Analysis of the experimental data show the presence of a critical Reynolds number that distinguish the drag increase and drag reduction regions. It has been postulated that the drag is the result of increased flow resistance due to increased extensional viscosity and the reduced form drag due to the influence of additives on vortex shedding and boundary layer separation. The experimental data of drag coefficient is best correlated with the polymer-particle parameter ϕ or Weissenberg number W_s as well as Reynolds number.

NOMENCLATURE.

- A buoyancy force; $A = g \cdot \rho_p \cdot (D_p)^2 \cdot \pi / 6$
Ar Archimedes number; $Ar = (D_p)^2 \cdot g \cdot (\rho / \mu)^2 / (\rho_p / \rho - 1)$
C polymer concentration in wppm (part per million by weight).
 C_D drag coefficient, $C_D = D / (\frac{1}{2} \rho U^2 \cdot (D_p)^2 \cdot \pi / 4)$
 C_{Dw} drag coefficient for Newtonian fluid (water)
D drag force
 D_p particle's diameter
g gravitational acceleration
M molecular weight of polymer additives
R universal gas constant
Re Reynolds number; $Re = U \cdot D_p \cdot \rho / \mu$
T solution temperature.
U settling velocity of spherical particles.
W weight of the spherical particle; $W = g \cdot \rho_p \cdot (D_p)^2 \cdot \pi / 6$
 W_s Weissenberg number; $W_s = \theta \cdot U / D_p$
 δC_D change in drag coefficient due to polymer additives; $\delta C_D = 1 - C_D / C_{Dw}$
 θ relaxation time of polymer additive solutions; $\theta = 50 \mu_s \cdot [\mu] \cdot M / (RT)$
 μ dynamic viscosity
 μ_s dynamic viscosity of the solvent (water)
 $[\mu]$ intrinsic viscosity of polymer solutions
 ν kinematic viscosity. $\nu = \mu / \rho$
 ρ fluid's density.
 ρ_p particle's density
 ϕ polymer-particle parameter, $\phi = \theta \nu / D_p$.

REFERENCES.

- 1 Rabie, L. H. "Drag reduction in turbulent shear flow due to injected polymer solutions", PhD Thesis, Edinburgh University, U.K., (1978).
- 2 Virk, P.S., "Drag reduction fundamentals", AIChE J., 21, 625, (1975).
- 3 Poreh, H., et al, "Drag reduction in hydraulic transport of solids", J. of the ASCE, Hydraulic Division, April 1970, pp.903-909, (quoted from (7)).

- 4 Ghassemzadeh, M.R., and Carmi, S., "Drag reduction in flow of coal-oil suspensions", ASME, J. Fluids Engineering, Vol 104, 92, (1982).
- 5 Pollert, J., "Hydrotransport of fly ash-Water mixture and drag reduction", Proc. 2nd Int. Conf. on Drag Reduction, Cambridge, England paper B3, (1977)
- 6 Goida, J., "Drag reduction in hydraulic transport of coal in pipes", Proc. of 3rd. Int. Conf. on Drag Reduction, Univ. of Bristol, Bristol, England, Paper D2, (1984).
- 7 Matthys, E.F., Ahn, H., and Sabersky, R.H., "Friction and heat transfer measurements for clay suspensions with polymer additives", ASME trans, J. Fluids Engineering, 109, 307, (1987).
- 8 Clift, R., Grace, J.R., and Webber, M.E., "Bubbles, Drops and Particles" Academic Press, New York, (1978).
- 9 Brauer, H., "Movement of single particles in various flow fields", Advances in Transport Processes, Edited by Mujumdar, A., and Mashelkar, R.A., Vol. II, 352, (1980).
- 10 Lee, S.L., "Particle drag in a dilute turbulent two-phase suspension flow", Int. J. Multiphase Flow, Vol. 13, 247-256, (1987).
- 11 Gore, R. A., and Crowe, C.T., "Discussion of particle drag in a dilute turbulent two-phase suspension flow", Int. J. Multiphase Flow, Vol. 16 359-361, (1990).
- 12 Liu, D.Y., Anders, K., and Frohn, A., "Drag coefficient of single droplets moving in an infinite droplet chain on the axis of a tube", Int. J. Multiphase Flow, Vol. 14, 217-232, (1988).
- 13 Hetsroni, G., "Particles - Turbulence interaction", Int. J. Multiphase Flow, Vol. 15, 735-746, (1989).
- 14 Huang, L.J., and Ayyaswamy, P.S., "Drag coefficients associated with a moving drop experiencing condensation", ASME trans, J Fluids Eng., 109, 1003, (1987).
- 15 Ni, S., "Particle diffusivity in fully developed turbulent horizontal pipe flow of dilute air-solid suspensions", Int. J. Multiphase Flow, Vol. 16, 43-56, (1990).
- 16 Berlemont, A., Desjonqueres, P., Gouesber, G., "Particle Lagrangian simulation in turbulent flows", Int. J. Multiphase Flow, Vol. 16, 19-34, (1990).
- 17 Govan, A.H., "A simple equation for the diffusion coefficient of large particles in a turbulent gas flow", Int. J. Multiphase flow, Vol 15, 287-294, (1989)
- 18 Ruck, B., and Makiola, B., "Particle dispersion in a single-sided backward - facing step flow", Int. J. Multiphase Flow, Vol.14, 787-800 (1988).
- 19 Valentik, I., and Whitmore, R.L., "The terminal velocity of spheres in Bingham plastics", Brit. J. Appl. Phys., Vol 16, 1197-1203, (1965).
- 20 Du Plessis, P.M., and Ansely R.W., "Settling parameter in solid pipe-lining, J. of the pipeline Division, Proc. of Am. Soc. Civil Eng., Vol. 93, 1-17, (1967), (quoted from [22])
- 21 Pazwash, H., and Robertson, J.M., "Forces on bodies in Bingham fluids", J. Hydr. Research, Vol 13 No.1, 35-55, (1975), (quoted from [22])
- 22 Dedegil, M.Y., "Drag coefficient and settling velocity of particles in non Newtonian suspensions", ASME Trans, J Fluids Engineering, 109, 319 (1987).
- 23 Slattery I.C., and Bird R.B., "Non Newtonian flow past sphere", Chem. Eng. Science, Vol. 16, 231-241, (1961)

- 24 Kit, E., and Poreh, M., "Drag of circular cylinders in dilute polymer solutions", Proc. 2nd Int. Conf. on Drag Reduction, Cambridge, England paper F2, (1977).
- 25 James, D.F., and Gupta, O.P., "Drag on circular cylinders in dilute polymer solutions", Chem. Eng. Progress Sympos. series, Drag Reduction 67, 111, pp.62-73, (1971).
- 26 Fruman, P. D., Loiseau, G. and Sulmont, P., " Effets viscoelastiques dans les mesures des pressions statiques et d'arret", La Houille Blanche / No 5, 445-452, (1970).
- 27 Kato, H., and Mizuno, Y., "An experimental investigation of viscoelastic flow past a circular cylinder", JSME, Vol. 26, No. 214, 529, (1983).
- 28 Hoyt J.W., "effect of additives on fluid friction", Trans. ASME, 94D, 258, (1972).
- 29 Everage, A. E., and Gordon R J, "On stretching of dilute polymer solutions" , AlChE J. Vol 17, No. 5, pp 1257, (1971)

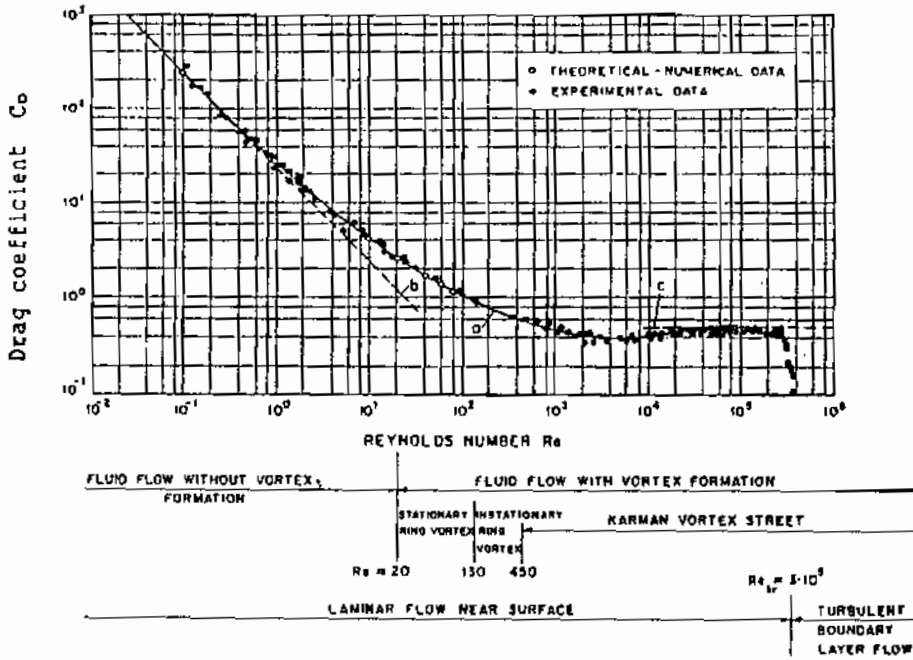


Figure (1)
 Typical plot of drag coefficient of spherical particles as function of Reynolds number (Figure is quoted from ref. [9]).

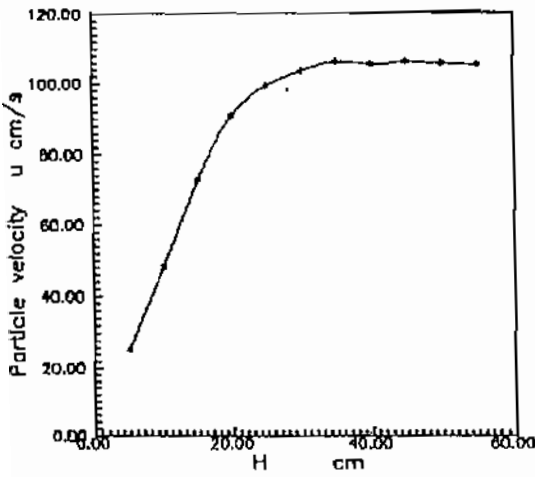


Figure (2)
 Particle fall velocity versus fall height in stagnant viscous fluid (water)

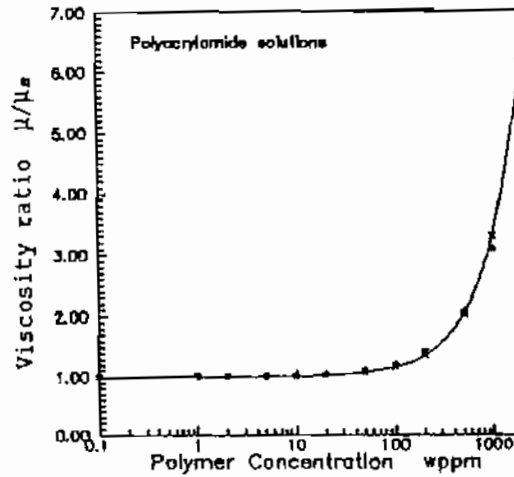


Figure (3)
 Ratio of Polyacrylamide solutions viscosity to that of water (μ/μ_w) versus polymer concentration

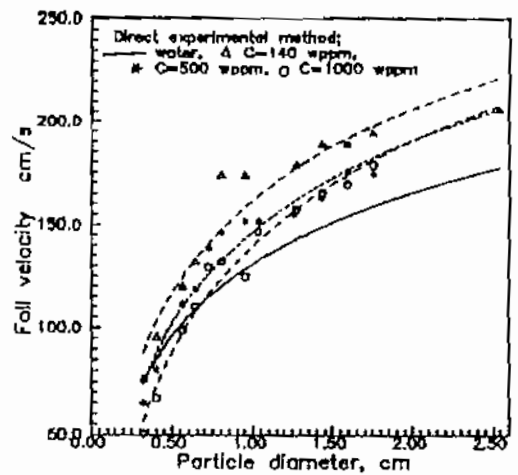
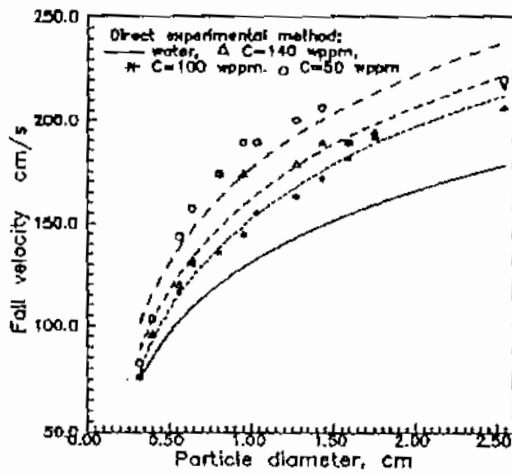
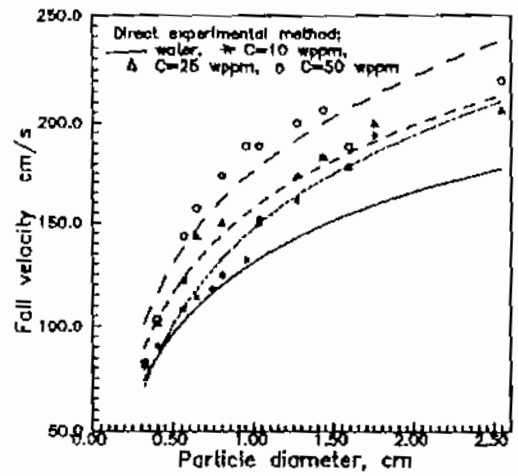
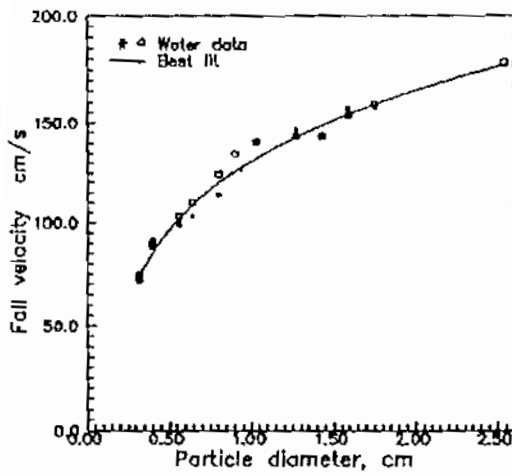
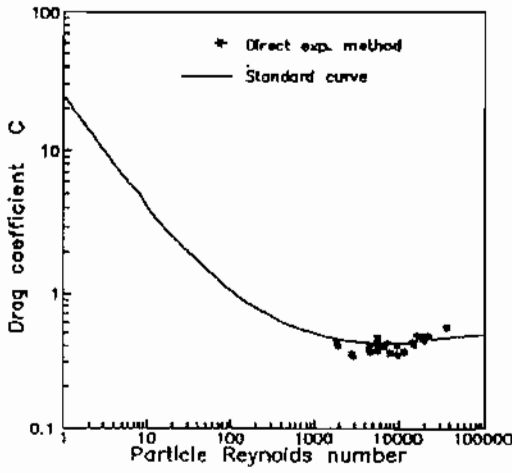
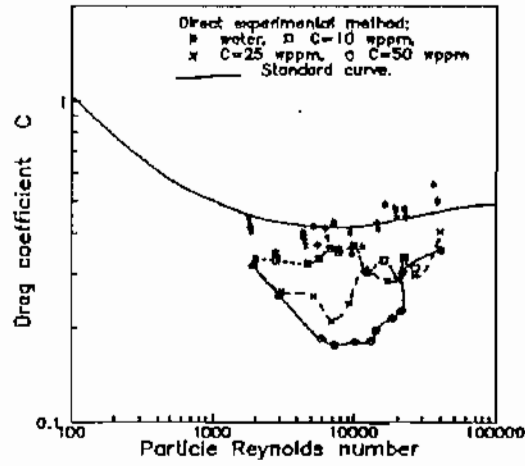


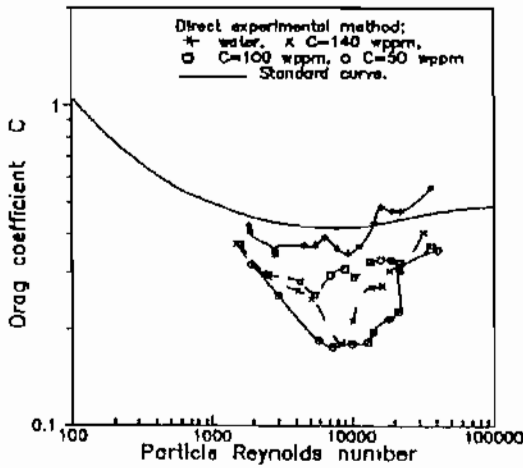
Figure (4)
Terminal fall velocity of spherical particles in Newtonian and drag reducing fluids versus particle's diameter.



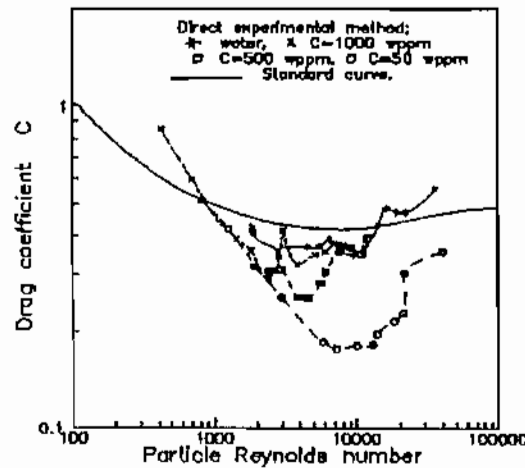
(5-a)



(5-b)



(5-c)



(5-d)

Figure (5)
Drag coefficient on spherical particles in Newtonian and drag reducing additive fluids versus Reynolds number.

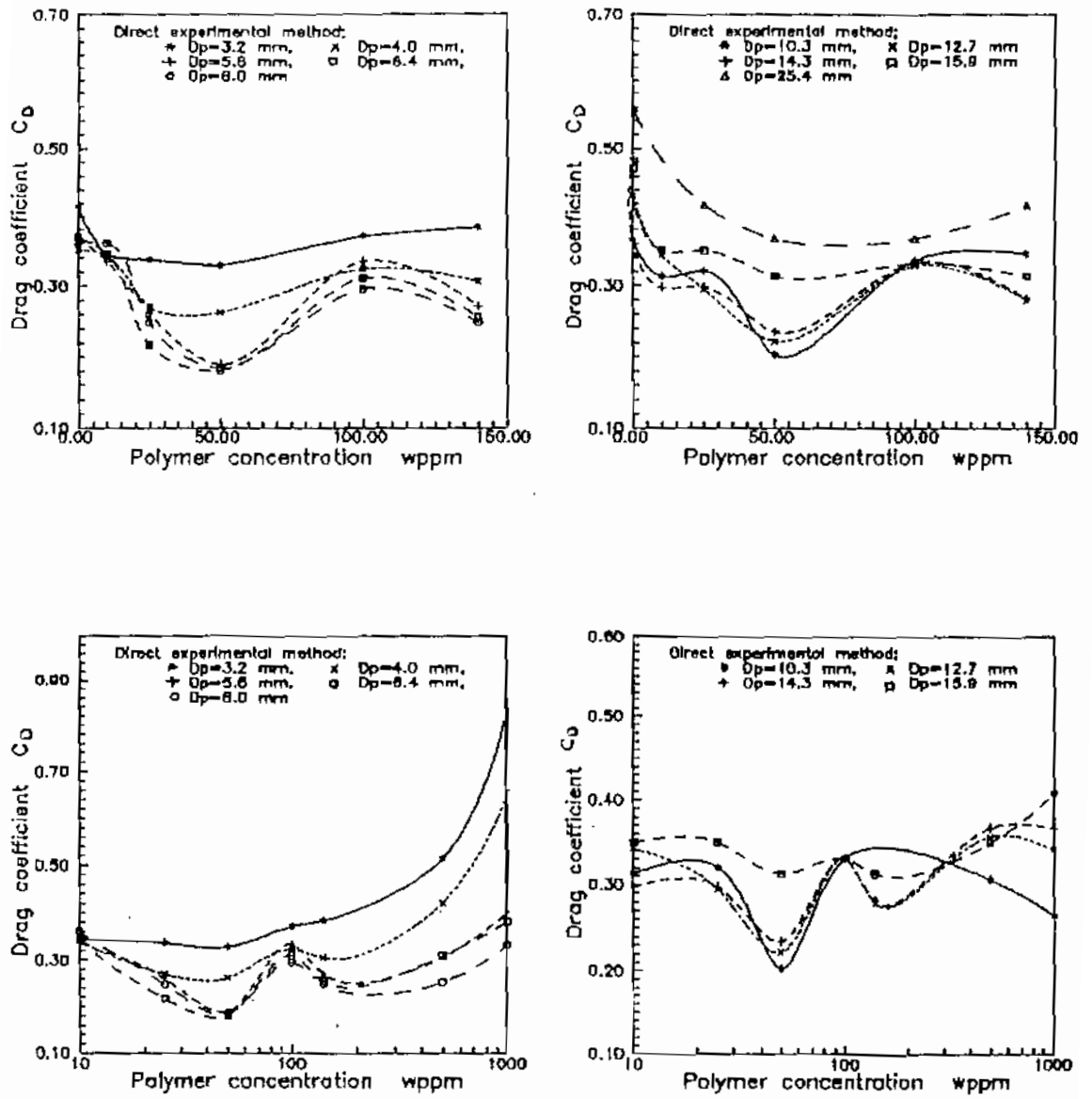


Figure (6)
 Drag coefficient on spherical particles in Newtonian and drag reducing additive fluids versus polymer concentration.

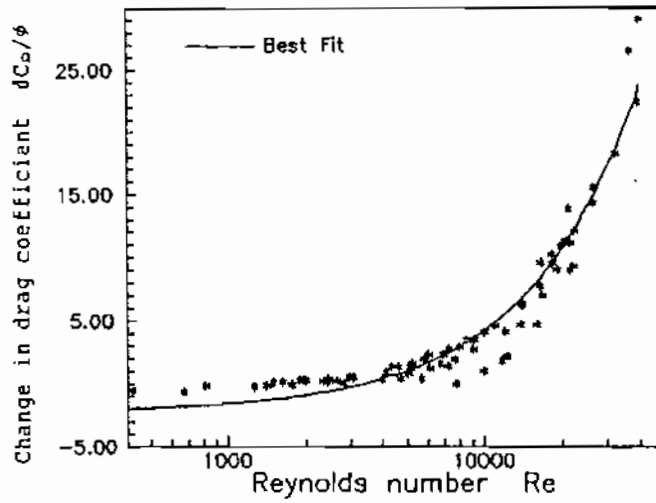


Figure (7)
Correlation of the change in particles drag coefficient due to drag reducing additives to polymer-particle parameter ϕ and particle's Reynolds number Re .

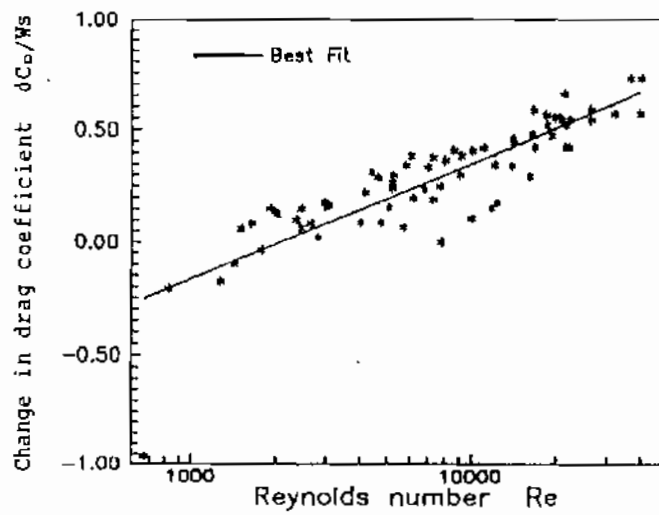


Figure (8)
Correlation of the change in particles drag coefficient due to drag reducing additives to Wessenberg number W_s and particle's Reynolds number Re .